small NANO MICRO

Biomineralization

Fabrication of Gold Nanoparticles Inside Unmodified Horse Spleen Apoferritin**

*Rongli Fan, Shu Wen Chew, Vee Vee Cheong, and Brendan Patrick Orner**

Inorganic nanomaterials have attracted extensive attention as a result of their emerging properties and their potential for a multitude of applications such as electronics, catalysis, sensors, and medical diagnosis.[1–3] With the hope of discovering novel properties for future applications, various methods have been developed to synthesize inorganic nanomaterials. The use of biological systems, inspired by naturally evolved processes, is an emerging trend in their fabrication, and it has been reported that material size, shape, and morphology can be controlled by interactions between biomolecules and inorganic materials.[4] Proteins and peptides, due to their large structural and functional diversity and their ready availability, have high utility in the manipulation of materials. Moreover, biotemplate-directed syntheses have the potential to be more "green" than traditional methods due to the required mild reaction conditions such as lower temperature, near-neutral pH, and the fact that they often employ aqueous reaction solutions. Proteins that assemble into nanocage structures have often been utilized as templates to produce many types of nanoparticles.[4]

The ferritin proteins assemble into robust nanoscale cages and are ubiquitously expressed in both prokaryotes and eukaryotes.[5–7] The ferritin protein from horse spleen, for example, is composed of 24 subunits that form an octahedral, hollow sphere with an exterior diameter of 12 nm and an interior cavity of 7 nm. The function of ferritin is to sequester and mineralize Fe(O)OH inside the cavity so as to prevent cytosolic and serum iron from forming cell-destructive, reactive oxygen species.[8,9] Iron is transported into the cavity through eight hydrophilic channels on the threefold symmetry axes and mineralized within the protein shell. It has been speculated that channels on the fourfold axes serve as exit pathways for cations during demineralization.[10]

Upon removal of their mineralized cores, empty cages of ferritin (i.e., apoferritin) have been used as size-constrained reaction vessels to synthesize different types of nanoparticles including metals,[11–16] oxides,[17–19] hydroxides,[20–22] carbonates,[23] and semiconductors.[24–29] These particles possess a narrow size distribution arising from growth restriction within the cage whose uniformity is a result of the precision of protein self-assembly. Moreover, it is thought that the protein cages could enhance the solubility and chemical stability of the particles. Therefore, multiple methods have been developed to mineralize nanoparticles using ferritins.[30] Many of the strategies have capitalized on natural electrostatic interactions or specific binding between metal ions and the interior surface of native ferritins[31,32] to increase the local concentration and thus facilitate the formation of nanoparticles. It has been assumed, due to the anionic nature of the ferritin cavity, and the direction of the electrostatic gradient in the ion-entry channels at the threefold axes, that only cations would be successful with this strategy. Other strategies respond to the fact that some metal ions have a natural affinity for the ferritin exterior, or in some cases no preference for either the interior nor exterior, resulting in substantial mineralization on the outside of the ferritin. In one remedy to this problem, ion-bound ferritins are first subjected to dialysis or chromatography before subsequent reduction inside the cavity.[15] Alternatively, ammonium ions, ethylenediaminetetraacetic acid (EDTA), or polyelectrolytes have been included in the reaction solution to retard or prevent mineralization on the outside of the cage.[21,23,26–28] Another strategy has been to genetically or chemically modify the proteins to endow the cavity with an enhanced ion binding affinity or the ability to promote particle formation.[12,13,16]

The mineralization of gold nanoparticles using ferritin cages was only recently reported in a series of two papers by Dmochowski et al. Reaction between either monoanionic $AuCl_4^-$ or neutral $AuCl_3$ and unmodified horse spleen apoferritin (HSAFn) resulted only in gold mineralization on the outside of the protein, and the size of these deposits could be controlled by the choice of the reductant.[33] In a subsequent report, human heavy chain ferritin was modified by removing solvent-exposed gold-binding amino acids, such as cysteine and histidine, from the outer surface and by lining the interior surface with cysteine residues. Gold nanoparticles were successfully incorporated inside the cavity of this modified protein by the addition of $AuCl_3$ followed by reduction with 3-(N-morpholino)propanesulfonic acid (MOPS).[16]

[*] Prof. B. P. Orner, R. Fan, S. W. Chew, V. V. Cheong
Division of Chemistry and Biological Chemistry
School of Physical and Mathematical Sciences
Nanyang Technological University
21 Nanyang Link 637371 (Singapore)
E-mail: orner@ntu.edu.s

[**] R.F. is supported by an SPMS graduate scholarship. S.W.C. thanks the CBC undergraduate final-year project fund. This research was supported by an SPMS start-up grant and a "Singapore Ministry of Education Academic Research Fund Tier 1 Grant" (RG 53/06). We thank Guo Jun from NTU's School of Materials Science and Engineering for helpful discussions regarding the diffraction data. We appreciate Prof. Chen Hongyu and Prof. Chen Yuan for use of their ultracentrifuge and we also thank Dr. Chen Gang and Wei Li for sucrose gradient centrifugation advice. We thank Ai Hua Seow for use of the CBC teaching-lab UV spectrometer.

Supporting Information is available on the WWW under http://www.small-journal.com or from the author.

DOI: 10.1002/smll.201000457

In this current work, we describe a novel strategy to mineralize gold nanoparticles inside native horse spleen apoferritin (HSAFn) without manipulating or modifying the protein shell. A challenge of this undertaking is that gold ions have a poor natural preference for the ferritin interior over that of the exterior, which thereby favors nanoparticle formation on the outside of the cage. Therefore, to encourage formation of particles only on the inside, we designed a strategy to trap a small number of gold ions inside the ferritin cavity and then isolate the encapsulated gold away from solution gold, which would have had the potential of mineralizing on the outside of the protein. Subsequently the entrapped gold ions could be rapidly reduced to form gold nanoclusters. Then in a second reduction step, additional gold ions could be added along with a weak reductant that preferentially permits mineralization on the nanocluster seed. The nanoparticle would grow until it matches the size of the inner cavity. A two-step reduction strategy such as this one should be amenable to nanoparticle growth inside almost any nanocage protein, and because final reduction occurs on a cluster, the production of particles with cores that are distinct from their shells should be possible. The challenges with this strategy are: 1) How to keep the initial number of gold ions low inside the ferritin so that the majority of the particle growth happens during the second reduction, 2) how to isolate the ferritin encapsulated ions and 3) how to control the selectivity of the reductions in each of the two steps.

To ensure that the number of gold ions is low inside the ferritin cage we use anionic $AuCl_4^-$ as the gold source as the interior of the protein cage is negatively charged. Moreover, calculations of the ferritin electrostatic potential reveal that the field at the threefold axis is directed through the channels toward the inside of the cavity presumably to facilitate the transport of cations.[10] Therefore, transport of gold anions into the cavity with a mechanism analogous to cations would be disfavored, thus ensuring a low number of gold ions present inside the cage. To isolate the ferritin-entrapped ions, we take advantage of protein biochemical techniques; size-exclusion chromatography is utilized to desalt the protein/gold ion solution since the method is able to isolate the protein with trapped ions in a mild way that keeps the protein cage intact. To control the reduction selectivity the first reduction was executed with the strong reductant, $NaBH_4$, to form small gold clusters (HSFn–Au clusters) while the second reduction on the gold clusters to fill up the protein cavities with gold nanoparticles (HSFn–AuNPs) was achieved with the mild reducing agent, ascorbic acid, which is unable to reduce gold in the absence of mineralized seeds (Figure 1).[34] To isolate pure and uniform-sized HSFn–AuNPs, gel filtration chromatography was applied to remove protein aggregations in the first purification step. Subsequently, another mild biochemical technique that separates based on density, ultracentrifugation through a sucrose gradient, was utilized to remove empty or incompletely mineralized ferritin. This mild, simple, and robust procedure yields highly homogeneous gold nanoparticles mineralized inside unmodified ferritin.

Characterization of the intermediates of our method was conducted by UV/vis spectroscopy (Figure 2). The spectra of HSAFn, HSFn–Au clusters, and HSFn–AuNPs all revealed strong absorbance at 280 nm primarily due to the presence of the protein. For the HSFn–AuNPs, an additional strong absorption peak at 519 nm was observed, indicating the characteristic surface plasmon resonance (SPR) of spherical gold nanoparticles less than 20 nm in diameter.[35,36] In contrast, the HSFn–Au clusters exhibited no identifiable SPR, suggesting that the size of the mineral cores was less than 2 nm in diameter.[37]

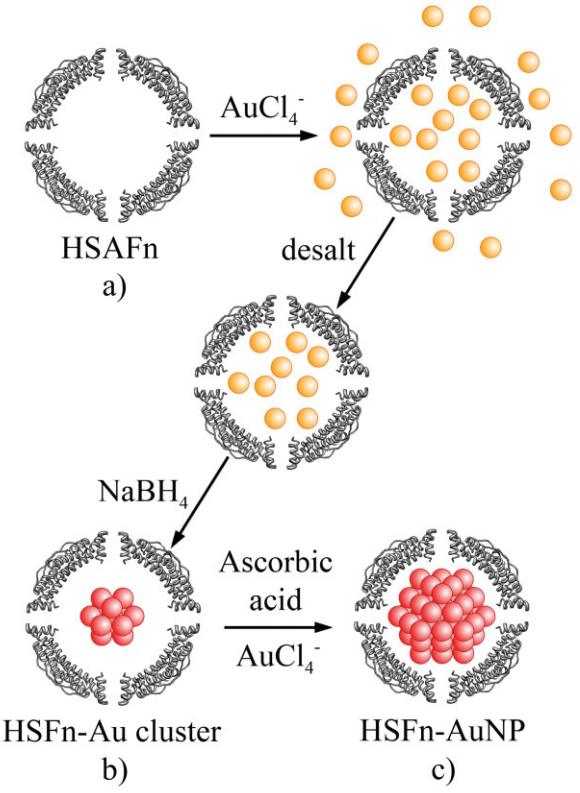

Figure 1. Schematic representation of the two-step procedure to use HSAFn to mineralize gold nanoparticles. Gold clusters (HSFn–Au clusters) are mineralized inside HSAFn by reducing $AuCl_4^-$ trapped inside the ferritin cavity. The formation of gold nanoparticles (HSFn–AuNPs) is promoted by addition of ascorbic acid and additional $AuCl_4^-$.

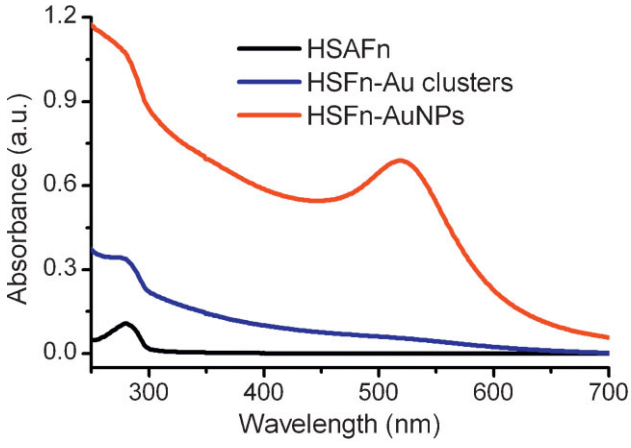

Figure 2. UV/vis spectra of horse spleen apoferritin (HSAFn, black), gold clusters mineralized in horse spleen ferritin (HSFn-Au clusters, blue) and gold nanoparticles mineralized in horse spleen ferritin (HSFn-AuNPs, red).

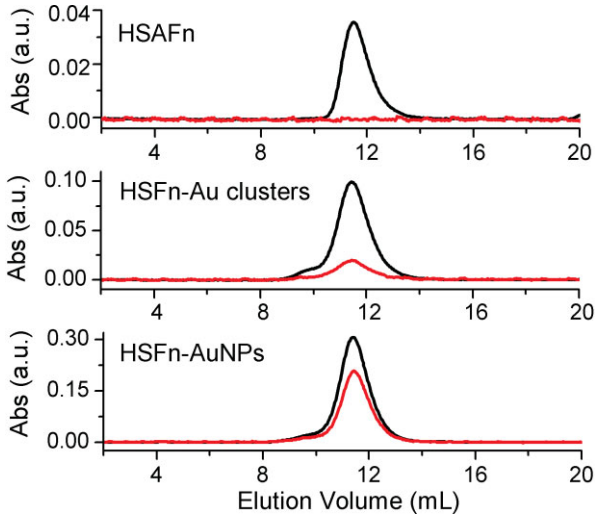

Figure 3. Size exclusion chromatography of horse spleen apoferritin (HSAFn, top), gold clusters mineralized in horse spleen ferritin (HSFn-Au clusters, middle), and gold nanoparticles mineralized in horse spleen ferritin (HSFn-AuNPs, bottom). Elution profiles were measured at 280 nm (black) and 520 nm (red).

Size exclusion chromatography (SEC) was performed to determine if the gold nanoparticles are associated with intact ferritins (Figure 3). Mineralized and non-mineralized proteins were monitored at 280 nm (protein) and 520 nm (gold nanoparticle). The unmineralized HSAFn eluted at 11.5 mL, which was consistent with a self-assembled 24-mer protein cage. As expected, it exhibited no peak when observed at 520 nm. The elution profiles monitored at 280 nm for both the HSFn–AuNPs and HSFn–Au clusters resulted in peaks with identical elution volumes as HSAFn, implying that the protein cages were intact and endured no major alterations during mineralization (Figure 3). In addition, the chromatograms of both HSFn–Au clusters and HSFn–AuNPs showed co-elution of protein and the presence of gold, suggesting that mineralization had occurred in association with the ferritin. Small shoulder peaks were observed in the elution profiles from both HSFn–Au clusters and the HSFn–AuNPs. These peaks were isolated and characterized and they proved to be the result of a small amount of protein aggregation formed during the reduction steps. This is not surprising as these conditions are, of course, non-native (Figure S1 of the Supporting Information).

To further confirm that the gold nanoparticles are indeed integrated with the protein shells, HSAFn and HSFn–AuNPs were electrophoresed in a native polyacrylamide gel (Figure 4). Both HSAFn and HSFn–AuNPs exhibited bands with the same electrophoretic mobility, suggesting that the overall charge of the ferritin was unchanged and the protein cage remained intact during the mineralization process. In addition, the band corresponding to HSFn–AuNPs was visibly red (indicating association between the protein and nanoparticles) prior to protein staining.

Transmission electron microscopy (TEM) with negative staining was conducted to visualize HSAFn, the HSFn–Au clusters, and the HSFn–AuNPs. The micrographs revealed that

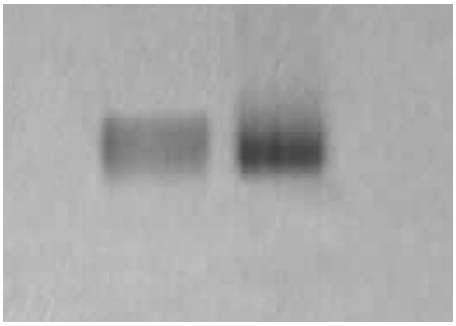

Figure 4. Native gel electrophoresis of horse spleen apoferritin (HSAFn, left) and gold nanoparticles mineralized in horse spleen ferritin (HSFn-AuNPs, right). Gel was stained with Coomassie blue.

HSAFn self-assembled into cagelike structures (Figure 5a) with an average diameter of 13.1 ± 0.7 nm, which was consistent with the literature (12 nm).[38] The HSFn–Au clusters were difficult to observe by TEM operating at 120 keV due to their small size and low electron density (Figure 5b); however, the HSFn–AuNPs could be visualized easily, and the gold nanoparticles appeared to be surrounded by intact protein shells (Figure 5c). In addition, the nanoparticles were monodisperse and spherical. The highly homogeneous population had an average diameter of 6.3 ± 0.8 nm, which is consistent with the interior dimension (7 nm)[38] of the protein cage, suggesting that the protein was responsible for controlling the size.

The elemental composition of the HSFn–AuNPs was determined using energy-dispersive X-ray (EDX) analysis (Figure 5d). The spectrum showed Mα, Lα, and Lβ, Au peaks (2.1, 9.7, and 11.4 keV respectively), which confirmed the presence of Au in the protein core. Moreover, a C peak (at 0.27 keV) and three Cu peaks (at 0.9, 8.0, and 8.9 keV) were observed, which are attributed to the protein shell and the TEM grid.

The structure of the nanoparticles mineralized in the ferritin was investigated at the atomic scale by high-resolution TEM (HRTEM). The micrograph (Figure 6a) shows an evident lattice indicating that the gold particles are single crystals. However, other micrographs of the HSFn–AuNPs indicate that some of them are polycrystalline (Figure S2 of the Supporting Information), suggesting that, in some cases, the gold crystals might be grown from one or more nucleation sites. Gold usually forms face-centered cubic (fcc) crystals. Measurement of the lattice spacings from the HRTEM image was 2.37 Å, corresponding to the value of the (111) facet of fcc gold crystals (2.36 Å). To further understand the crystal structure of the gold particles, selected-area electron diffraction (SAED) patterns from a large number of particles were obtained (Figure 6b). The observed *d*-spacings at 2.4, 2.1, 1.5, 1.3, and 0.97 Å correspond to miller indices of (111), (200), (220), (311), and (331) in fcc gold crystals respectively (Table 1).

After the HSFn–AuNPs were synthesized, gel filtration chromatography was applied to remove the protein aggregates. However, as this technique separates based on size differences, the resulting HSFn–AuNPs preparation had $40 \pm 3\%$ empty or incompletely mineralized ferritins (Figure S3a,b of the Supporting Information). A homogeneous preparation of

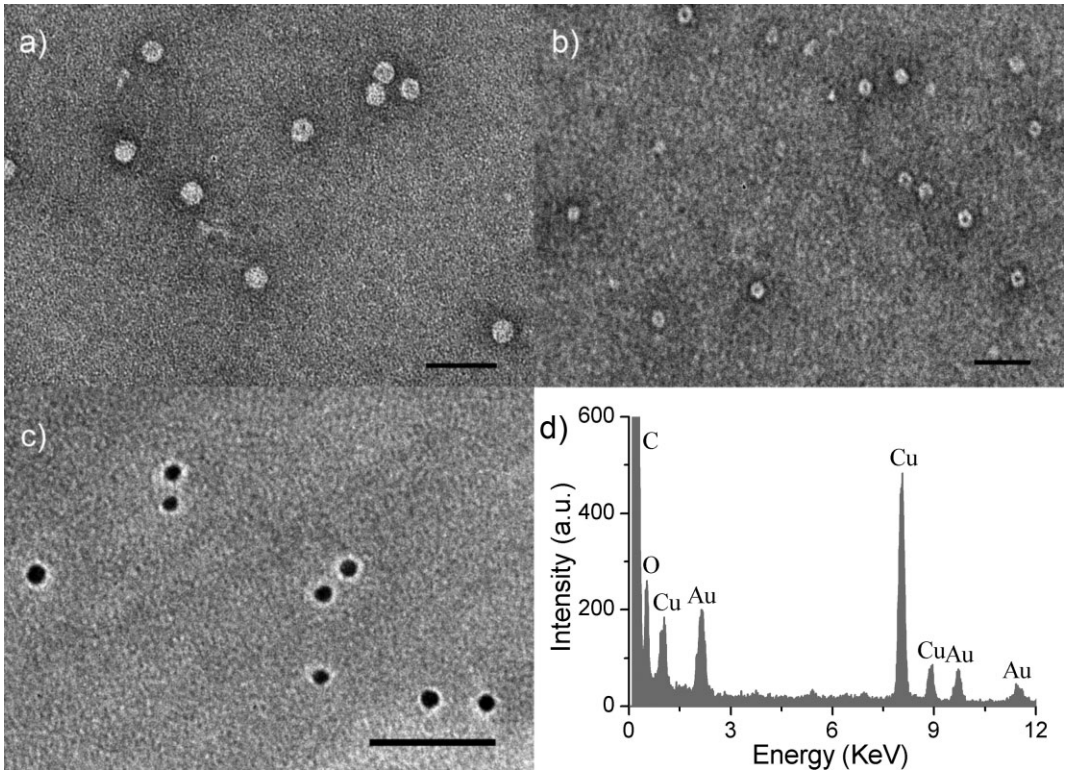

Figure 5. TEM images of a) negatively stained HSAFn, b) negatively stained HSFn-Au clusters, c) negatively stained HSFn–AuNPs. Each scale bar is 50 nm. d) EDX spectrum of unstained HSFn–AuNPs. The spectrum was obtained on a copper grid.

HSFn–AuNPs was obtained after sucrose gradient ultracentrifugation, which resulted in $94 \pm 2\%$ of the ferritins filled with nanoparticles with an average diameter of 6.3 ± 0.8 nm (Figure S3c–f of the Supporting Information).

To verify the necessity of both reduction steps in our fabrication procedure we designed a control experiment to determine whether clusters were present after desalting but before the first reduction. If they were, treating them with ascorbic acid and $AuCl_4^-$ should result in nanoparticles fully filling the protein cavity. This experiment gave rise to a deep-blue solution after only a few minutes, and TEM visualization indicated that only large, non-uniform gold structures were formed (Figure S4 of the Supporting Information). This result suggests that either there are no gold nanoclusters formed until the initial reduction or that some sort of clusters exist both before and after the first reduction, but they are not the same species. Moreover, this experiment emphasizes that both reduction steps are indeed essential.

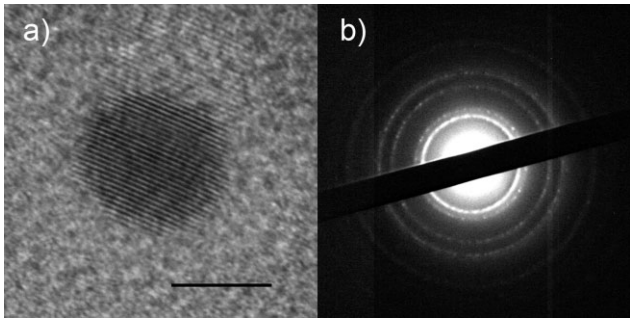

Figure 6. a) HRTEM image and b) SAED pattern for unstained gold nanoparticles mineralized in horse spleen ferritin. The scale bar in (a) is 5 nm and the camera length for (b) is 20 cm.

In conclusion, we report a new two-step method to produce gold nanoparticles inside ferritin protein cages that requires no modification of the protein. The formation of nanoparticles on the exterior could be suppressed by first loading gold anions into the cage followed by removal of the excess ions in solution immediately before reacting with the first reductant. The resulting clusters are then used to seed nanoparticle formation by slow reduction. We confirmed that highly monodisperse nanocrystals are formed within intact protein shells and the size of the nanoparticles correlates with the interior diameter of the cages. Gold nanoparticles are of immense interest due to their multiple applications[36] and our mild and flexible fabrication method could aid in that research. In addition, the protein surface could be easily modified through chemical and genetic methods to direct other functions for further applications. We also think that our approach to first form clusters within the protein cages to nucleate nanoparticle growth could be used to

Table 1. Theoretical and observed *d*-spacings for gold nanoparticles mineralized in horse spleen ferritin.

d-spacing [Å]	Measured *d*-spacing [Å]	hkl
2.4	2.4	111
2.0	2.1	200
1.4	1.5	220
1.2	1.3	311
0.94	0.97	331

synthesize core/shell or alloy nanoparticles inside ferritins. Finally, the fact that our procedure does not require any modification of the protein means that it could be readily amenable to any cage protein whether they are altered structural variants of the ferritins[39] or viruses.

Experimental Section

HSAFn was obtained from Sigma–Aldrich and purified by fast protein liquid chromatography (FPLC, GE Healthcare) using gel filtration (Superdex 200 10/300 GL, 50 mM sodium phosphate, 150 mM NaCl, pH 7.0). Protein concentration was determined by bicinchoninic acid (BCA). Purified HSAFn (1 mL of a 1 mg mL^{-1} solution) was mixed with $HAuCl_4$ (22.6 μL of a 0.1 M solution; protein: $HAuCl_4$ molar ratio of 1: 1000). The resulting homogeneous, pale-yellow solution was incubated at room temperature for 3 h and applied to a desalting column (Sephadex G-25, 50 mM tris buffer, pH 7.5). The fractions containing protein were combined (1.5 mL) and $NaBH_4$ (20 μL of a 0.1 M solution) was added. The solution was inverted slowly for 10 min before unagitated incubation at room temperature for 3 h to water quench the remaining hydride. To the resulting light-reddish–brown solution, freshly dissolved ascorbic acid (30 μL of a 0.1 M solution) and $HAuCl_4$ (10 μL of a 0.1 M solution) were added, and it was incubated with no agitation overnight at room temperature. The resulting ruby-red solution was centrifuged (10000 rpm, 10 min) and the supernatant was purified by gel filtration (Superdex 200 10/300 GL, 50 mM sodium phosphate, 150 mM NaCl, pH 7.0). To isolate a homogeneous preparation of the HSFn–AuNPs, the sample was then applied to 20% to 60% sucrose gradient and centrifuged at 40000 rpm for 5 h. The bottom layer was collected and subjected to buffer exchange (50 mM tris, pH 7.5).

HSAFn, HSFn–Au clusters, and HSFn–AuNPs (100 μg mL^{-1}) were analyzed by gel filtration (Superdex 200 10/300 GL, 50 mM sodium phosphate, 150 mM NaCl, pH 7.0) with monitoring at 280 nm (for protein) and 520 nm (for gold particles). UV/vis spectra of samples (100 μg mL^{-1}) were recorded on a Cary 100 spectrophotometer from 700 nm to 250 nm. Samples were analyzed by native polyacrylamide gel electrophoresis with 4% stacking gel and 7% resolving gel and staining with Coomassie blue. TEM of all samples was obtained on a JEOL JEM-1400 microscope operating at 120 keV and negative stained with methylamine tungstate (Nano-W, Nanoprobes, Yaphank, NY). Particle sizes were determined by image analysis (Image J., National Institutes of Health, USA, $n = 100$). Data from HRTEM, EDX, and SAED were obtained by using a JEOL JEM-2100F operating at 200 keV.

Keywords:

biomineralization · encapsulation · gold · nanomaterials · proteins

[1] A. N. Shipway, E. Katz, I. Willner, *ChemPhysChem* **2000**, *1*, 18.
[2] N. L. Rosi, C. A. Mirkin, *Chem. Rev.* **2005**, *105*, 1547.
[3] I. Yamashita, *J. Mater. Chem.* **2008**, *18*, 3813.
[4] M. B. Dickerson, K. H. Sandhage, R. R. Naik, *Chem. Rev.* **2008**, *108*, 4935.
[5] S. Mann, F. C. Meldrum, *Adv. Mater.* **1991**, *3*, 316.
[6] F. C. Meldrum, V. J. Wade, D. L. Nimmo, B. R. Heywood, S. Mann, *Nature* **1991**, *349*, 684.
[7] P. M. Harrison, P. Arosio, *Biochim. Biophys. Acta Bioenergetics* **1996**, *1275*, 161.
[8] H. N. Munro, M. C. Linder, *Physiolog. Rev.* **1978**, *58*, 317.
[9] E. C. Theil, *Ann. Rev. Biochem.* **1987**, *56*, 289.
[10] T. Douglas, D. R. Ripoll, *Protein Sci.* **1998**, *7*, 1083.
[11] T. Ueno, M. Suzuki, T. Goto, T. Matsumoto, K. Nagayama, Y. Watanabe, *Angew. Chem. Int. Ed.* **2004**, *43*, 2527.
[12] R. M. Kramer, C. Li, D. C. Carter, M. O. Stone, R. R. Naik, *J. Am. Chem. Soc.* **2004**, *126*, 13282.
[13] M. T. Klem, D. Willits, D. J. Solis, A. M. Belcher, M. Young, T. Douglas, *Adv. Funct. Mater.* **2005**, *15*, 1489.
[14] J. M. Dominguez-Vera, N. Galvez, P. Sanchez, A. J. Mota, S. Trasobares, J. C. Hernandez, J. J. Calvino, *Eur. J. Inorg. Chem.* **2007**, 4823.
[15] N. Galvez, B. Fernandez, E. Valero, P. Sanchez, R. Cuesta, J. M. Dominguez-Vera, *C. R. Chim.* **2008**, *11*, 1207.
[16] C. A. Butts, J. Swift, S. G. Kang, L. Di Costanzo, D. W. Christianson, J. G. Saven, I. J. Dmochowski, *Biochemistry* **2008**, *47*, 12729.
[17] R. Tsukamoto, K. Iwahor, M. Muraoka, I. Yamashita, *Bull. Chem. Soc. Jap.* **2005**, *78*, 2075.
[18] F. C. Meldrum, B. R. Heywood, S. Mann, *Science* **1992**, *257*, 522.
[19] M. Allen, D. Willits, J. Mosolf, M. Young, T. Douglas, *Adv. Mater.* **2002**, *14*, 1562.
[20] T. Douglas, V. T. Stark, *Inorg. Chem.* **2000**, *39*, 1828.
[21] M. Okuda, K. Iwahori, I. Yamashita, H. Yoshimura, *Biotechnol. Bioeng.* **2003**, *84*, 187.
[22] M. T. Klem, J. Mosolf, M. Young, T. Douglas, *Inorg. Chem.* **2008**, *47*, 2237.
[23] M. Li, C. Viravaidya, S. Mann, *Small* **2007**, *3*, 1477.
[24] K. K. W. Wong, S. Mann, *Adv. Mater.* **1996**, *8*, 928.
[25] K. Iwahori, T. Enomoto, H. Furusho, A. Miura, K. Nishio, Y. Mishima, I. Yamashita, *Chem. Mater.* **2007**, *19*, 3105.
[26] I. Yamashita, J. Hayashi, M. Hara, *Chem. Lett.* **2004**, *33*, 1158.
[27] R. M. Xing, X. Y. Wang, L. L. Yan, C. L. Zhang, Z. Yang, X. H. Wang, Z. J. Guo, *Dalton Trans.* **2009**, 1710.
[28] K. Iwahori, K. Yoshizawa, M. Muraoka, I. Yamashita, *Inorg. Chem.* **2005**, *44*, 6393.
[29] B. Hennequin, L. Turyanska, T. Ben, A. M. Beltran, S. I. Molina, M. Li, S. Mann, A. Patane, N. R. Thomas, *Adv. Mater.* **2008**, *20*, 3592.
[30] H. Yoshimura, *Colloids Surf. A* **2006**, *282*, 464.
[31] A. Treffry, P. M. Harrison, *J. Inorg. Biochem.* **1984**, *21*, 9.
[32] B. Webb, J. Frame, Z. Zhao, M. L. Lee, G. D. Watt, *Arch. Biochem. Biophys.* **1994**, *309*, 178.
[33] L. Zhang, J. Swift, C. A. Butts, V. Yerubandi, I. J. Dmochowski, *J. Inorg. Biochem.* **2007**, *101*, 1719.
[34] N. R. Jana, L. Gearheart, C. J. Murphy, *J. Phys. Chem. B* **2001**, *105*, 4065.
[35] K. L. Kelly, E. Coronado, L. L. Zhao, G. C. Schatz, *J. Phys. Chem. B* **2003**, *107*, 668.
[36] M. C. Daniel, D. Astruc, *Chem. Rev.* **2004**, *104*, 293.
[37] C. Burda, X. B. Chen, R. Narayanan, M. A. El-Sayed, *Chem. Rev.* **2005**, *105*, 1025.
[38] P. M. Harrison, S. C. Andrews, P. J. Artymiuk, G. C. Ford, J. R. Guest, J. Hirzmann, D. M. Lawson, J. C. Livingstone, J. M. A. Smith, A. Treffry, S. J. Yewdall, *Adv. Inorg. Chem.* **1991**, *36*, 449.
[39] R. L. Fan, A. L. Boyle, V. V. Cheong, S. L. Ng, B. P. Orner, *Biochemistry* **2009**, *48*, 5623.

Received: March 18, 2010

